

UKAEA-CCFE-PR(21)82

J. R. Harrison, T. Farley, G. M. Fishpool, A. Kirk, B. Lipschultz, J. Lovell, F. Militello, D. Moulton, P. Ryan, R. Scannell, A. J. Thornton, K. Verhaegh, L. Xiang

Initial observations of divertor heat flux mitigation in the Super-X divertor configuration in MAST Upgrade

Enquiries about copyright and reproduction should in the first instance be addressed to the UKAEA Publications Officer, Culham Science Centre, Building K1/O/83 Abingdon, Oxfordshire, OX14 3DB, UK. The United Kingdom Atomic Energy Authority is the copyright holder.

The contents of this document and all other UKAEA Preprints, Reports and Conference Papers are available to view online free at scientific-publications.ukaea.uk/

Initial observations of divertor heat flux mitigation in the Super-X divertor configuration in MAST Upgrade

J. R. Harrison, T. Farley, G. M. Fishpool, A. Kirk, B. Lipschultz, J. Lovell, F. Militello, D. Moulton, P. Ryan, R. Scannell, A. J. Thornton, K. Verhaegh, L. Xiang

Initial demonstration of enhanced divertor heat flux mitigation and detachment access in the MAST Upgrade Super-X divertor configuration

J. R. Harrison¹, T. Farley¹, G. M. Fishpool¹, A. Kirk¹, B. Lipschultz², J. Lovell³, F. Militello¹, D. Moulton¹, P. Ryan¹, R. Scannell¹, A. J. Thornton¹, K. Verhaegh¹, L. Xiang¹

¹ United Kingdom Atomic Energy Authority, Culham Centre for Fusion Energy, Culham Science Centre, Abingdon, Oxon, OX14 3DB, UK

² York Plasma Institute, Department of Physics, University of York, Heslington, York YO10 5DD, United Kingdom

³ Oak Ridge National Laboratory, Oak Ridge, TN 37831, USA

Abstract

The predicted benefits of an optimised Super-X divertor configuration in mitigating the steady-state power and particle fluxes to the surfaces of the MAST Upgrade divertor have been demonstrated experimentally for the first time. In the attached parallel transport regime, the divertor heat flux is a factor ~ 10 lower in the Super-X configuration. The core density required to access the detached divertor regime was reduced by a factor 2 in the Super-X configuration, in good agreement with modelling predictions. In the operating conditions reported herein, there was no significant impact by Super-X divertor operation on the plasma core temperature and density profiles, and hence energy confinement.

One of the most significant challenges facing the development of fusion energy is to safely spread the power from fusion-born alpha particles over surfaces within the reactor. That would ensure that the heat fluxes arising from particles and energy escaping the hot fusion core that impinge on surfaces within a fusion device can be tolerated by materials without causing excessive damage, erosion or reducing the lifetime of the surfaces. For example, in an EU DEMO reactor [1], more than 95% of the power heating the plasma (from fusion reactions and auxiliary heating) needs to be dissipated before reaching the surfaces of the device as plasma. Otherwise, excessive fluxes of particles and heat to these surfaces can result in them being damaged with consequences including reducing the availability of the plant due to repair or replace damaged components.

The deposited power flux density from the plasma to divertor targets, q_{dep} , can be expressed as [2]:

$$q_{dep} = (\gamma_{sh} k_B T_{e,t} + E_{pot}) \Gamma \sin \theta = q_{\parallel} \sin \theta \quad (1)$$

where γ_{sh} is the sheath heat transmission coefficient, Γ is the particle flux parallel to the magnetic field, T_e is the electron temperature, E_{pot} is the potential energy released per ion as it recombines to form molecules, q_{\parallel} is the plasma heat flux parallel to the magnetic field ($\gamma_{sh} k_B T_{e,t} \Gamma$) and θ is the angle between magnetic field lines and the divertor surface, which is typically at least $1-3^\circ$ due to engineering constraints. Substantial reductions in this power flux can be achieved through promoting radiative losses from the plasma through fuelling hydrogenic and/or impurity gases and innovative divertor designs to reduce T_e . Further reductions in this power flux can only be achieved by reducing the divertor particle flux, $\Gamma \left(\propto p_e / \sqrt{T_e} \right)$ where p_e is the electron pressure, by inducing significant pressure loss from the plasma via collisions with neutrals in the so-called “detached” regime [3] when T_e is very low, typically below $\sim 5\text{eV}$ [4]. Consequently, operating in this regime is mandatory for ITER [5] to moderate divertor power loads and in future reactors to reduce erosion of divertor plasma-facing surfaces [6, 7]. However, it is normally observed in devices with conventional divertors that the means used to reach detached divertor conditions can result in some degradation of confinement of the core plasma (e.g. [8, 9, 10]). Significantly improving access to the detached divertor regime is challenging, for example, increasing closure of a conventional divertor has been observed to reduce the detachment threshold by only 15-25% on MAST Upgrade and other devices (e.g. [11, 12]).

Alternative divertor configurations offer potential solutions to the power exhaust challenge (see [13] and references therein) by increasing the area over which the exhaust power is deposited and potentially enhancing dissipation of heat, pressure and particles via improved access to the detached divertor regime compared with conventional divertors. The Super-X alternative divertor configuration [14] has the distinctive feature that the divertor targets are situated at large major radius (R_T), and hence lower magnetic field, thereby reducing the surface heat fluxes by increasing the surface area ($\propto R_T$). Moreover, the poloidal field in divertor volume is reduced using magnetic coils to increase the length of field lines in the divertor to reduce T_e via heat conduction [15] and potentially increase radiation losses. A significant predicted benefit of the Super-X configuration in MAST Upgrade is a factor ~ 2 reduction in the electron density at the outer mid-plane required to detach the outer divertors [16, 17, 18, 15]. This significantly broadens the operational space of a device where effective mitigation of divertor power loads occurs, thus facilitating its integration with a high-performance core, including suppression of ELMs [19]. In spherical tokamaks such as MAST Upgrade [20, 21], it is predicted that the strong gradients in the magnetic field across the divertor, and concomitant gradients in $q_{\parallel}(\propto |B|)$, can lead to improved control of divertor detachment [18] as these gradients passively make the detachment “front” less sensitive to external control.

Extensive simulations were performed to study the benefits of the Super-X vs conventional divertor configurations in MAST Upgrade [22, 23, 17], in simplified geometry [16] and compared with analytic calculations [18, 15]. They confirmed that the benefits of the Super-X configuration, in terms of substantially reduced outer divertor surface power loads and improved access to the detached divertor regime. In experiments, these predictions were tested in plasmas with identical plasma current, heating power and core plasma shape in the L-mode confinement regime with conventional and Super-X divertor configurations, as shown in Figure 1. The magnetic topology is a connected double null configuration with up-down symmetry about the plane at $Z = 0$ m to maximise the power to the outer divertors [24]. In this optimised Super-X divertor configuration, the distance along magnetic field lines from the outer mid-plane to outer divertor targets was doubled compared with the conventional divertor. This was achieved by moving the strike point out in major radius by a factor ~ 2 (thereby halving the magnetic field at the target, and hence q_{\parallel}) and reducing the poloidal field B_{pol} in the divertor chambers, which increases the poloidal flux expansion ($f_{exp} \propto 1/B_{pol}$) and decreases θ by a factor 4-5. The overall geometrical expansion of the divertor footprint can be quantified as the area expansion, the ratio of annular area of the outer divertor targets between adjacent flux surfaces compared with the area at the outer mid-plane $\left(\frac{R_T+0.5\Delta R_T}{R_{mp}+0.5\Delta R_{mp}}\right) f_{exp}$ where R_{mp} is the major radius of the outer mid-plane, ΔR_T and ΔR_{mp} are the radial separation between adjacent flux surfaces at the divertor target and outer mid-plane respectively. In the Super-X configuration, this area expansion is a factor ~ 9 higher than the conventional divertor due to the increased strike point major radius and poloidal flux expansion.

The outer divertor heat flux profiles to the lower outer divertor were measured by IR thermography with sufficient spatial coverage to monitor the surface temperature of the divertor tiles in conventional and Super-X divertor configurations and derive the incident heat fluxes. Using gas fuelling from the main chamber, the core electron density was varied for both divertor configurations to study the impact of proximity to divertor detachment on these power loads, as shown in Figure 2. This range of densities spans 10-35% of the Greenwald density limit [25]. Over this range in density, the power crossing the separatrix is relatively constant, at 500-600 kW. Both conventional and Super-X divertor configurations have good neutral trapping, with the outer strike points situated below the gas baffles that effectively trap recycling particles within the divertor chambers. At the lowest densities studied, the peak heat flux to the outer divertor was around a factor 10 lower in the Super-X configuration compared with the conventional. At higher densities, the peak heat flux reduces monotonically with increasing density in the conventional divertor configuration. However, the initially low heat flux in the Super-X configuration at low core density drops below the detection threshold of the diagnostic at higher densities as the divertor detaches, thereby preventing an estimation of divertor heat flux reduction after the onset of detachment.

Quantification of the detachment threshold in upstream density was performed by monitoring the ion flux profiles to the outer divertors measured using Langmuir probes as the core density is increased to observe a characteristic “roll over” in the divertor target integrated ion flux with increasing density at detachment onset. To facilitate a fair comparison, only data taken from the first 100ms of the Super-X divertor phase was used where the gas pressure in the closed divertor volume should not vary significantly and is relatively low. Later in the pulse, the gas pressure in the Super-X configuration is likely to be higher which would further reduce the detachment threshold. These data, shown in Figure 3, are in good agreement with earlier modelling predictions [23, 17] that

the upstream density required to detach the outer divertors is a factor ~ 2 lower in the MAST-U Super-X configuration compared with the conventional. Following the onset of detachment, both divertor configurations exhibit a similarly rapid reduction in the outer divertor ion flux with increasing density and these observations will be combined with measurements of the movement of emission fronts in hydrogenic and impurity spectral lines to discern whether the front position is more amenable to external control.

The significant flexibility to vary the magnetic configuration in MAST Upgrade allows for the direct comparison of conventional and Super-X divertor configurations in otherwise very similar core plasma conditions and shaping. High resolution profiles of the electron temperature and density across the core plasma core have been measured with Thomson scattering over the full range of densities explored in this study which suggest that these profiles are not significantly affected by the variation in divertor configuration. Moreover, a comparison of these profiles at a line average density of $1.1 \times 10^{19} \text{ m}^{-3}$, shown in Figure 4, are very similar despite the divertor in the Super-X configuration being in the detached regime and the conventional being attached. Similar observations are found when comparing the outer divertor ion flux profiles in the two divertor conditions at similar core line average density, which exhibit a similar shape when compared in poloidal flux space, accounting for the differences in poloidal flux expansion shown in Figure 1.

In conclusion, the beneficial properties of an optimised Super-X divertor configuration have been quantified in experiments and modelling, showing very good agreement. In the attached divertor regime, the divertor power loads are reduced by a factor ~ 10 in the Super-X configuration compared with an otherwise identical conventional divertor by expanding the area over which the power is deposited through nearly doubling the major radius of the strike points and increasing the poloidal width of the divertors. At higher core densities, the threshold density required to reach the detached regime is reduced by a factor ~ 2 in the Super-X configuration. Despite the presence of significantly lower divertor power loads and detachment access in the Super-X configuration, there was no significant change in the confinement of the core plasma in L-mode.

Acknowledgements

We would like to thank the enormous efforts of the MAST-U tokamak technical and research staff in bringing the machine and accompanying diagnostics to operation, resulting in the results presented. We also thank Mike Kotschenreuther and Swadesh Mahajan from the Institute for Fusion Studies, University of Texas for useful discussions on the Super-X divertor configuration. This work was funded by the RCUK Energy Programme [grant number EP/T012250/1]. To obtain further information on the data and models underlying this paper please contact PublicationsManager@ukaea.uk.

References

- [1] M. Wischmeier et al., *J. Nucl. Mater.* **463** 22-29 (2015)
- [2] A. Loarte et al., *Nucl. Fusion* **47** S203-263 (2007)
- [3] G. F. Matthews N. *Nucl. Mater.* **220-222** 104-116 (1995)
- [4] A. W. Leonard *Plasma Phys. Control. Fusion* **60** 044001
- [5] R. A. Pitts et al., *Nucl. Mater. Energy* **20** 100696 (2019)
- [6] G. Federici et al., *Nucl. Fusion* **57** 092002 (2017)
- [7] M. Siccino et al., *Nucl. Fusion* **59** 106026 (2019)
- [8] A. Kallenbach et al., *Nucl. Fusion* **55** 053026 (2015)
- [9] J. A. Goetz et al., *Phys. Plasmas* **6** 1899 (1999)
- [10] M. Bernert, *Nucl. Mater. Energy* **12** 111-118 (2017)
- [11] A. L. Moser et al., *Nucl. Mater. Energy* **19** 67-71 (2019)
- [12] O. Février et al., *Nucl. Mater. Energy* **27** 100977 (2021)
- [13] V. A. Soukhanovskii *Plasma Phys. Control. Fusion* **59** 064005 (2017)
- [14] P. M. Valanju, M. Kotschenreuther, S. Mahajan, J. Canik *Phys. Plasmas* **16** 056110 (2009)
- [15] T. W. Petrie et al., *Nucl. Fusion* **53** 113024 (2013)
- [16] D. Moulton, J. Harrison, B. Lipschultz, D. Coster, *Plasma Phys. Control. Fusion* **59** 065011 (2017)
- [17] J. R. Harrison et al., *Nucl. Fusion* **59** 112011 (2019)
- [18] B. Lipschultz, F. I. Parra, I. H. Hutchinson *Nucl. Fusion* **56** 056007 (2016)
- [19] A. Kallenbach et al., *Nucl. Fusion* **57** 102015 (2017)
- [20] G. Fishpool et al., *J. Nucl. Mater.* **438** S356-S359 (2013)
- [21] A. W. Morris et al., *IEEE Trans. Plasma Sci.* **46** 5 1217-1226 (2018)
- [22] E. Havlíčková et al., *Plasma Phys. Control. Fusion* **56** 075008 (2014)
- [23] E. Havlíčková et al., *Plasma Phys. Control. Fusion* **57** 115001 (2015)
- [24] G. De Temmerman et al., *Plasma Phys. Control. Fusion* **52** 095005 (2010)
- [25] M. Greenwald *Plasma Phys. Control. Fusion* **44** R27–R80 (2002)

Figures

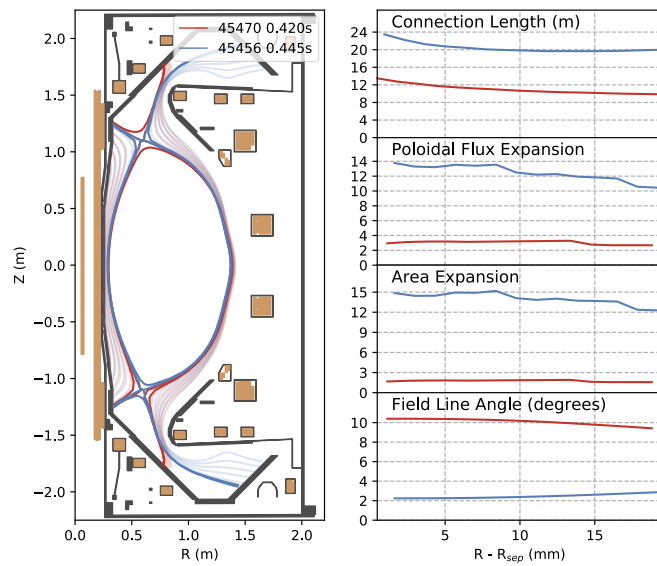


Figure 1: Left - Conventional (red) and Super-X (blue) divertor configurations on MAST Upgrade. Right – magnetic properties of the conventional and Super-X configurations that can facilitate access to detachment in the Super-X (due to longer field line connection length from the outer mid-plane to outer divertor target and higher poloidal flux expansion) and reduce divertor power loads via increasing the area over which power is deposited in the divertor through increased area expansion.

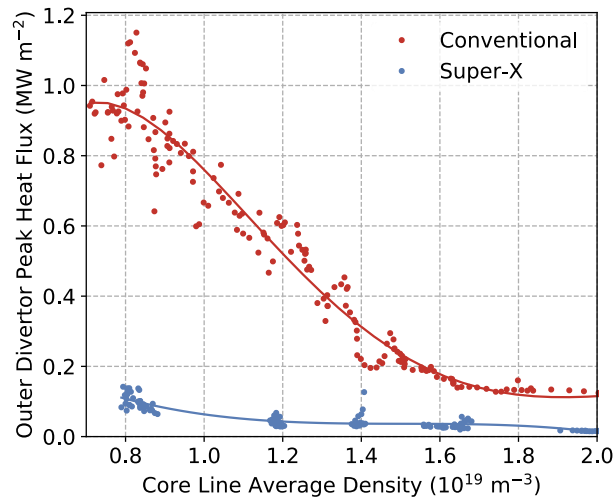


Figure 2: Dependence of the outer divertor heat flux with increasing core line average density in the conventional (red) and Super-X (blue) configurations with smoothed curves overlaid. At the lowest densities, the peak heat flux to the outer divertor is a factor 10 lower than in the conventional configuration.

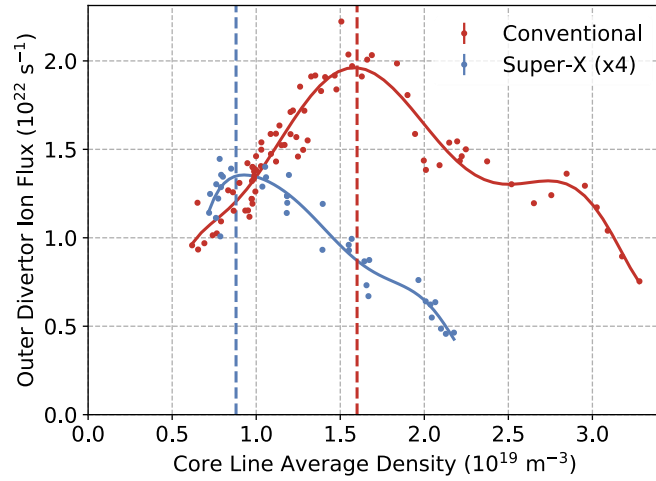


Figure 3: Dependence of the outer divertor ion flux with increasing core line average density in the conventional (red) and Super-X (blue) configurations with smoothed curves overlaid (solid). The point where the divertor ion flux stops increasing with rising core line average density, emblematic of the onset of detachment, is highlighted by dashed vertical lines, showing a factor ~ 2 reduction in the density required to detach the outer divertor in the Super-X configuration.

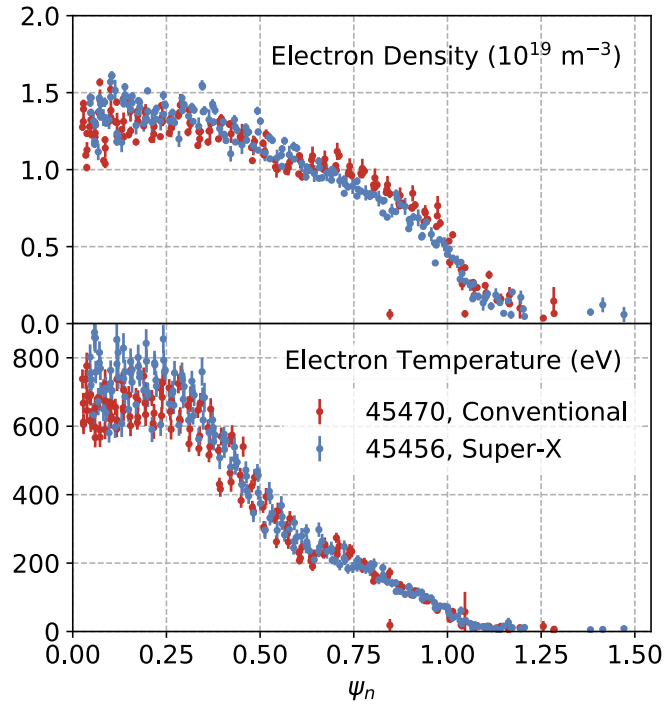


Figure 4: Core plasma profiles of electron density (top) and electron density (bottom) in experiments with conventional (red) and Super-X (blue) configurations with similar core line-average density. Despite the differences in divertor configuration and the Super-X being in the detached divertor regime and the conventional is attached at this density, there is negligible impact on these core profiles.